J. Aerosol Sci., Vol. 20, No. 3, pp. 355–366, 1989.
Printed in Great Britain.

0021-8502/89 $3.00 + 0.00

DEPOSITION OF FIBERS IN THE RAT LUNG

B. ASGHARIAN and C. P. YU

State University of New York at Buffalo Amherst, NY 14260, U.S.A.

(*Received* 18 *May* 1988, *and in final form* 21 *September* 1988)

Abstract—The deposition and clearance of inhaled particles in the lungs of different mammals have been the subject of many investigations. Any analysis on the particle removal from the lung requires a knowledge of the initial deposition pattern of inhaled particles at different sites. In this study, a deposition model is employed in conjunction with the data of the airway geometry to calculate the deposition of fibers at various locations in the rat lung. In the process, the simultaneous effect of Brownian rotation and velocity shear on the fiber orientation is considered. The results show that although long fibers are effectively filtered by the airways in the head and tracheobronchial regions, a smaller fraction of those fibers can penetrate into the pulmonary region and deposit there. The calculated results compared favorably with the experimental data of Morgan *et al.* (*Inhaled Particles* IV. Pergamon Press, Oxford, 1977) and Hammad *et al.* (*Ann. occup. Hyg.* **26**, 179–187, 1982).

INTRODUCTION

Inhalation of asbestos fibers has been recognized to produce lung diseases in humans and animals (Wagner *et al.*, 1974; Davis *et al.*, 1978). Due to the health hazards involved, experimentation on human subjects is not feasible and only post-mortem studies were made in which little is known about the exposure condition. On the other hand, under controlled conditions, many experiments have been conducted on rats and other animals. In these experiments, fibers are administered into the lung either by instillation through the trachea or by inhalation exposure for an extended period. The animals are then killed and the amount of fiber retention in the lung and the degree of lung injury are observed (e.g. Morgan *et al.*, 1977; Hammad *et al.*, 1982; Pinkerton *et al.*, 1984). These procedures have proved useful to the process of finding a quantitative relationship between fiber exposure and lung disease.

It is generally believed that lung disease is a result of the inability of the lung to remove the deposited particles effectively. A preliminary step in determining the retention of particles in the lung is to find the initial deposition pattern. In this paper, a theoretical model is developed to study the deposition of fibers in the rat lung. To validate the theoretical model, the computed deposition results are compared with available experimental data from several studies.

COLLECTION EFFICIENCIES IN THE AIRWAYS

The amount of deposition of fibers in an airway depends strongly upon their orientation with respect to the direction of air flow. There are two mechanisms which determine the fiber orientation: the velocity shear in the flow and Brownian rotation. At a given location, the orientation of fibers, expressed by an orientation distribution function, $P(\phi, \theta, t)$, is governed by the Fokker–Planck equation

$$\frac{\partial P}{\partial t} + \nabla \cdot (\omega P - {}^{r}D \cdot \nabla P) = 0, \tag{1}$$

with

$$\int_{\phi=0}^{2\pi} \int_{\theta=0}^{\frac{\pi}{2}} P(\phi, \theta, t) \sin\theta \, d\theta \, d\phi = 1, \tag{2}$$

where ω is the angular velocity of fiber rotation, ${}^{r}D$ is the Brownian diffusion coefficient for rotation, and ϕ and θ are the Eulerian angles shown in Fig. 1.

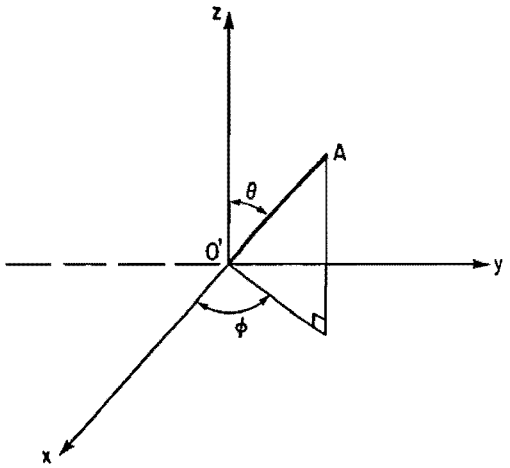

Fig. 1. Orientation of a fiber.

Uncharged fibers can deposit on the airway surface by the mechanisms of diffusion, sedimentation, impaction and interception. The deposition efficiencies of these mechanisms have been derived by extending the results of spherical particles to fibers except for interception (Asgharian and Yu, 1988a).

A. *Diffusion*

For diffusional deposition of fibers in a parabolic flow, the efficiency is

$$\eta_d = \{1 - 0.819\exp(-14.63\Lambda) - 0.097\exp(-89.22\Lambda) - 0.0325\exp(-228\Lambda) - 0.0509\exp(-125.9\Lambda^{2/3})\}, \quad (3)$$

where

$$\Lambda = \frac{L'D}{4UR^2}, \quad (4)$$

in which L and R are, respectively, the airway length and radius, U is the average velocity in the airway, and $'D$ is the translational diffusion coefficient of fibers, given by

$$'D = kT\int_{r^*=0}^{1}\int_{\phi=0}^{2\pi}\int_{\theta=0}^{\pi}\frac{C_F(d_e)P(r^*,\phi,\theta)}{f^0}\sin\theta\,d\theta\,d\phi\,dr^*, \quad (5)$$

where $P(r^*, \phi, \theta)$ is the orientation distribution of fibers, k is the Boltzmann constant, T is the absolute temperature, $r^* = r/R$ with r being the radial distance from the axis of the airway, f^0 is the drag per unit velocity in the continuum regime, and C_F is the Cunningham correction factor which has the form

$$C_F = 1 + \mathrm{Kn}\left[C_1 + C_2\exp\left(-\frac{C_3}{\mathrm{Kn}}\right)\right], \quad (6)$$

where $C_1 = 1.142$, $C_2 = 0.558$ and $C_3 = 0.999$ for solid particles (Allen and Raabe, 1985), and Kn is the Knudsen number, defined by

$$\mathrm{Kn} = \frac{2\lambda}{d_e}, \quad (7)$$

in which λ is the mean free path of the air molecules and d_e is the equivalent diameter for slip correction (Asgharian and Yu, 1988b).

B. *Sedimentation*

The collection efficiency of fiber sedimentation in a parabolic flow through a horizontal tube is

$$\eta_s=\frac{2}{\pi}(2\varepsilon\sqrt{1-\varepsilon^{2/3}}-\varepsilon^{1/3}\sqrt{1-\varepsilon^{1/3}}+\sin^{-1}\varepsilon^{1/3}), \tag{8}$$

where

$$\varepsilon=\frac{3u_gL}{8UR}, \tag{9}$$

in which u_g is the fiber terminal settling velocity. The average settling velocity for a system of fibers with an orientation distribution $P(r^*, \phi, \theta)$ is then

$$\bar{u}_g=\frac{2}{\pi}\int_{\alpha=0}^{\frac{\pi}{2}}\int_{r^*=0}^{1}\int_{\phi=0}^{2\pi}\int_{\theta=0}^{\pi}P(r^*, \phi, \theta)u_g(\phi, \theta)\sin\theta\,d\theta\,d\phi\,dr^*\,d\alpha, \tag{10}$$

where α is the angle between the line connecting the center of the fiber to the center of the airway cross-section and the horizontal. For an airway with an inclination angle, γ, with the horizontal, equation (9) should be modified by replacing u_g with $u_g\cos\gamma$, and upon substitution of $\bar{u}_g$ from equation (10) into (9) for u_g, the sedimentation efficiency of fibers in a system of randomly oriented airways can be obtained by integration with respect to γ. The result is

$$\bar{\eta}_s=\int_{\gamma=0}^{\frac{\pi}{2}}\eta_s(\gamma)\cos\gamma\,d\gamma. \tag{11}$$

C. *Impaction*

Impaction efficiency is the fraction of fibers deposited at the bifurcation of an airway due to their inertia. The impaction efficiency of fibers was found to be (Yu *et al.*, 1986)

$$\eta_{imp}=0.768\,\mathrm{St}\,\theta_b, \tag{12}$$

where θ_b is the bend angle and St is the fiber Stokes number. For a system of fibers with an orientation distribution $P(r^*, \phi, \theta)$, St in equation (12) is replaced by the average Stokes number, $\overline{\mathrm{St}}$, given by

$$\overline{\mathrm{St}}=\int_{r^*=0}^{1}\int_{\phi=0}^{2\pi}\int_{\theta=0}^{\pi}P(r^*, \phi, \theta)\,\mathrm{St}(\phi, \theta)\sin\theta\,d\theta\,d\phi\,dr^*. \tag{13}$$

D. *Interception*

Because of their elongated geometry, fibers can also deposit at the carina of a bifurcation by direct interception. Asgharian and Yu (1989) obtained the following expression for the interception efficiency of fibers at an airway bifurcation:

$$\eta_{int}=\frac{1}{2\pi}\int_{\phi=0}^{2\pi}\int_{\theta=0}^{\frac{\pi}{2}}I(\phi, \theta)\sin\theta\,d\theta\,d\phi, \tag{14}$$

where

$$I(\phi, \theta)=\frac{8}{\pi}\int_{\Gamma=0}^{\Gamma'}\int_{r^*=0}^{\frac{l_p\sin(\Gamma-\Omega)}{2R\cos\Gamma}}P(r^*, \phi, \theta)r^*(1-r^{*2})\,dr^*\,d\Gamma$$

$$+\int_{\Gamma=\Gamma'}^{\frac{\pi}{2}}\int_{r^*=0}^{r_0'}P(r^*, \phi, \theta)r^*(1-r^{*2})\,dr^*\,d\Gamma, \tag{15}$$

in which

$$\Gamma' = \cos^{-1}\left(\frac{l_p}{2R}\cos\Omega\right), \tag{16}$$

$$l_p = l_f(1-\sin^2\theta\sin^2\phi)^{\frac{1}{2}}, \tag{17}$$

$$\Omega = \cos^{-1}\left(\frac{l_f\cos\theta}{l_p}\right), \tag{18}$$

$$r^{*\prime} = \frac{l_p\sin(\Gamma'-\Omega)}{2R\cos\Gamma'}, \tag{19}$$

and l_f and l_p are, respectively, the fiber length and its projection on the plane of the airway cross-section.

E. *Approximate solution*

It is clear that the above formulas for the collection efficiencies require the knowledge of $P(r^*, \phi, \theta)$. Peterlin (1938) considered the problem of suspended ellipsoidal particles in a constant shear flow and solved the Fokker–Planck equation (1) to obtain a steady state solution in the form

$$P(\phi,\theta) = \frac{1}{4\pi}\left\{1 + \frac{3\Delta\sin^2\theta}{1+\left(\frac{6}{{}^r\mathrm{Pe}}\right)^2}\left(-\frac{1}{2}\cos 2\phi + \frac{3}{{}^r\mathrm{Pe}}\sin 2\phi\right)\right.$$
$$+\frac{\Delta^2}{1+\left(\frac{6}{{}^r\mathrm{Pe}}\right)^2}\left[-\frac{3}{14}(3\cos^3\theta-1)+\frac{9}{560}(35\cos^4\theta-30\cos\theta+3)\right.$$
$$\left.\left.+\frac{15\sin^4\theta}{16\left(1+\frac{100}{{}^r\mathrm{Pe}^2}\right)}\left(\cos 4\phi\left(1-\frac{60}{{}^r\mathrm{Pe}^2}\right)-\frac{16}{{}^r\mathrm{Pe}}\sin 4\phi\right)\right]+\Delta^3[\ldots]\right\}, \tag{20}$$

where

$$\Delta = \frac{\beta^2-1}{\beta^2+1}, \tag{21}$$

β is the aspect ratio of the fiber, and ${}^r\mathrm{Pe}$ is the rotational Peclet number, defined by

$${}^r\mathrm{Pe} = \frac{G}{{}^rD}, \tag{22}$$

in which G is the velocity gradient and ${}^rD$ is the rotational diffusion coefficient.

Equation (20) can be applied locally to a parabolic flow in a tube for which the velocity gradient is a function of the radial position. Since this equation is a series solution of Δ, a rapid convergence requires $\Delta \ll 1$, which corresponds to small values of β. For large β, as Δ approaches unity, many terms in equation (20) are required to calculate $P(\phi, \theta)$. To avoid this difficulty, an alternative approach was used in calculating collection efficiencies.

We assume that the collection efficiency of fibers due to each mechanism is a linear combination of two separate efficiencies, one for the case of random fiber orientation and another for the orientation as determined from the periodic rotation solution of fibers resulting from the velocity shear, i.e.

$$\eta = f_1({}^r\mathrm{Pe})\eta_P + f_2({}^r\mathrm{Pe})\eta_R, \tag{23}$$

where η_P and η_R are, respectively, the collection efficiencies of fibers in periodic rotation and random orientation, and the weighting functions f_1 and f_2 are assumed to have the form

$$f_1 = \frac{({}^r\mathrm{Pe})^b}{a+({}^r\mathrm{Pe})^b}, \tag{24}$$

and

$$f_2 = \frac{a}{a + ({}^r\mathrm{Pe})^b}, \tag{25}$$

where ^{r}Pe is the rotational Peclet number defined in equation (22) with $G = U/R$, and a and b are constants. Equation (23) reduces, obviously, to the correct limiting results of η at both $^r\mathrm{Pe} = 0$ and $^r\mathrm{Pe} = \infty$. For intermediate values of ^{r}Pe, it was shown (Asgharian and Yu, 1989) that equation (23) yielded a good approximation to the exact result of η calculated by using equation (20) if $a = 50$ and $b = 1.5$.

Since various deposition mechanisms are independent of each other, the total average fractional loss of fibers in an airway due to all mechanisms per unit length of the airway, λ, can be obtained by superposition. The result is

$$\lambda = \frac{1}{L}(\bar{\eta}_s + \eta_{\mathrm{imp}} + \eta_d + \eta_{\mathrm{int}}). \tag{26}$$

COLLECTION EFFICIENCY IN THE HEAD REGION

In the laboratory experiments, rats are often exposed by nasal inhalation. Deposition in the nose is by impaction and interception. Experimental data show that efficiency by impaction, N_{imp}, is proportional to the particle Stokes number. We assume a functional relationship in the form

$$N_{\mathrm{imp}} = C_4 + C_5 \log \rho_0 d_{ei}^2 Q, \tag{27}$$

where ρ_0 is the unit mass density, d_{ei} is the equivalent diameter for impaction when the fibers are oriented randomly, Q is the flow rate through the nose, and C_4 and C_5 are coefficients obtained by fitting equation (27) with the data of Raabe *et al.* (1975) measured for spherical particles in the nose of rats. Using the first degree least square method for the best fit, C_4 and C_5 are found to be 0.089 and 0.1158, respectively.

Because of the lack of data, interception deposition by nasal hairs in rats is neglected in this work. For small fiber lengths, the deposition results will not be affected whereas for long ones, some changes in the results are expected.

REGIONAL AND TOTAL DEPOSITION

Equations (26) and (27) were utilized in a deposition model (Yu and Diu, 1983) to calculate the deposition of fibers in the rat. The lung model employed in this calculation is the one reported by Yeh (1980). In addition, we assume a distribution of alveoli in the unciliated airways in the lung model similar to that found in humans (Weibel, 1963). The lung volume of the rat used in the calculation is 10.78 cm^3. The tidal volume is 1.68 cm^3 and the breathing frequency is 98 cycles min^{-1} with equal time for inhalation and exhalation and no pause.

The deposition in each lobe of the rat lung is studied first. The tidal volume is assumed to be distributed in each lobe proportional to the lung volume of that lobe. A fiber diameter of $d_f = 0.2$ μm with different lengths is used in the calculation. The mass density of the fiber, ρ, is taken to be 3.37 g cm^{-3}. The calculated deposition results are shown in Table 1. We see that the depositions in the right apical, right cardiac and right intermediate lobe are about equal and they are less than half of the depositions in the right diaphragmatic and left lung lobe. This tendency is similar to that found for spherical particles (Schum and Yeh, 1980). Shown in the last two columns of Table 1 are the summation of the lobar depositions and the deposition results calculated from the whole lung model. The results of the whole lung model are found to be slightly smaller than the summation of the lobar ones for all fiber lengths. In the remainder of this study, we shall only present the results from the whole lung model for various discussions.

The deposition fraction is defined as the number of fibers deposited divided by the total number of fibers inhaled. The results of deposition fraction in the nose are shown in Fig. 2 for

Table 1. Percent deposition in the rat lung for fibers with $d_f = 0.2\ \mu m$, $\rho = 3.37\ g\,cm^{-3}$ at a lung volume of $10.78\ cm^3$, a tidal volume of $1.68\ cm^3$ and a breathing frequency of 98 cycles min^{-1}

Length (μm)	Region	R.A.	R.C.	R.I.	R.D.	L.L.	C.S.	Sum	W.L.
0.5	TB	0.176	0.223	0.28	0.805	0.796	0.17	2.45	2.28
	P	0.356	0.308	0.386	0.894	0.904	–	2.85	2.41
1	TB	0.172	0.222	0.289	0.838	0.797	0.19	2.51	2.31
	P	0.299	0.257	0.32	0.735	0.748	–	2.36	1.99
5	TB	0.308	0.389	0.55	1.50	1.33	0.27	4.25	3.91
	P	0.25	0.21	0.264	0.598	0.613	–	1.94	1.62
10	TB	0.416	0.507	0.755	0.198	0.166	0.27	5.58	4.93
	P	0.267	0.222	0.279	0.624	0.652	–	2.04	1.69

TB = Tracheobronchial, P = pulmonary, R.A. = right apical lobe, R.C. = right cardiac lobe, R.I. = right intermediate lobe, R.D. = right diaphragmatic lobe, L.L. = left lung lobe, C.S. = common stem segments, and W.L. = whole lung model.

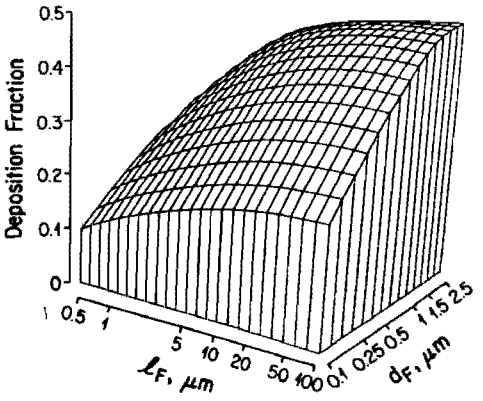

Fig. 2. Deposition of fibers in the nose with $\rho = 3.37\ g\,cm^{-3}$.

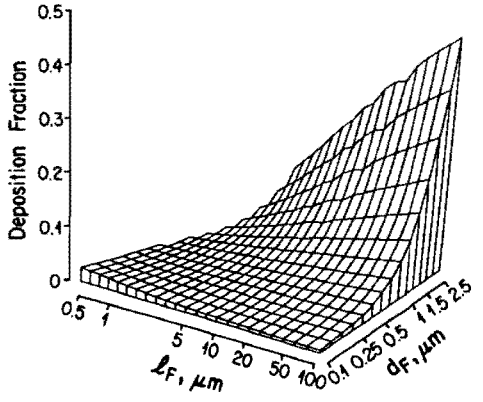

Fig. 3. Tracheobronchial deposition via trachea with no interceptional deposition at a lung volume of $10.78\ cm^3$, a tidal volume of $1.68\ cm^3$, a breathing frequency of 98 cycles min^{-1} and $\rho = 3.37\ g\,cm^{-3}$.

different fiber diameters and lengths. It is seen that deposition fraction increases more rapidly with the fiber diameter than with the fiber length which implies that the aerodynamic behavior of a fiber depends more strongly on its diameters.

Figure 3 shows the deposition fraction of fibers in the tracheobronchial region when fibers enter the lung via the trachea. For the purpose of gaining a better understanding of the deposition mechanisms, interceptional deposition is neglected in this figure. As we can see,

deposition is mainly by impaction for thick fibers and some diffusion for thin fibers. Sedimentation deposition of thick fibers is not important in this region of the lung because of the high flow rate. In the impaction-dominated fiber size range, deposition increases rapidly with the fiber diameter and slightly with the fiber length as we previously observed in the nose. At small fiber diameters where diffusion is dominant, deposition decreases as the fiber length increases.

Shown in Fig. 4 is the deposition in the tracheobronchial region when the interceptional deposition is included. The contribution of the interceptional deposition is apparent. The results in Fig. 4 also show that long fibers deposit more in the tracheobronchial region; thin ones by interception and thick ones by both impaction and interception.

The deposition fraction results in the tracheobronchial region via nose breathing are shown in Fig. 5. The deposition pattern for constant diameter is similar to Fig. 4. However, because of the filtering effect of the nose, deposition fraction for constant length shows a minimum value at some diameter.

Fibers that escape deposition in the nose and the tracheobronchial region will penetrate into the pulmonary region. The deposition results for fibers which enter the lung via the trachea when the interceptional deposition is excluded are shown in Fig. 6. In the absence of interception, sedimentation and diffusion are the controlling deposition mechanisms since the flow in the pulmonary region is slow. At small fiber diameters, diffusional deposition is noticeable for short fibers and decreases as the fiber length increases. When the fiber diameter increases, deposition increases rapidly due to increasing sedimentation. At large diameters, there is only a moderate increase of deposition with the fiber length.

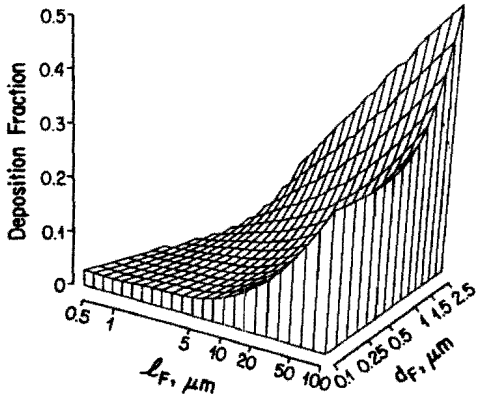

Fig. 4. Tracheobronchial deposition via trachea at a lung volume of 10.78 cm^3, a tidal volume of 1.68 cm^3, a breathing frequency of 98 cycles min^{-1} and $\rho = 3.37\ g\,cm^{-3}$.

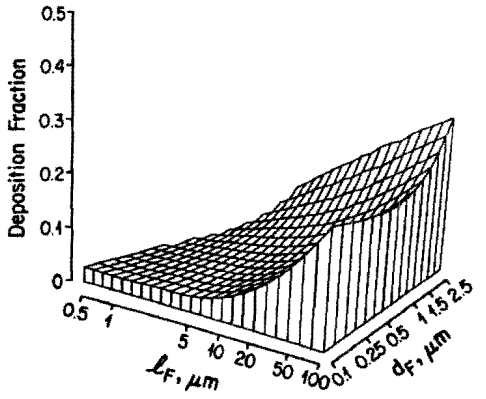

Fig. 5. Tracheobronchial deposition via nose breathing at a lung volume of 10.78 cm^3, a tidal volume of 1.68 cm^3, a breathing frequency of 98 cycles min^{-1} and $\rho = 3.37\ g\,cm^{-3}$.

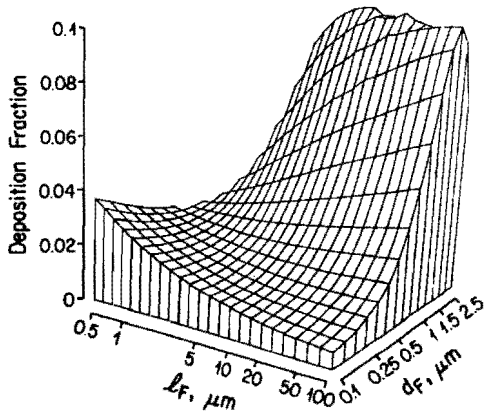

Fig. 6. Pulmonary deposition via trachea with no interceptional deposition at a lung volume of 10.78 cm^3, a tidal volume of 1.68 cm^3, a breathing frequency of 98 cycles min^{-1} and $\rho = 3.37\ g\,cm^{-3}$.

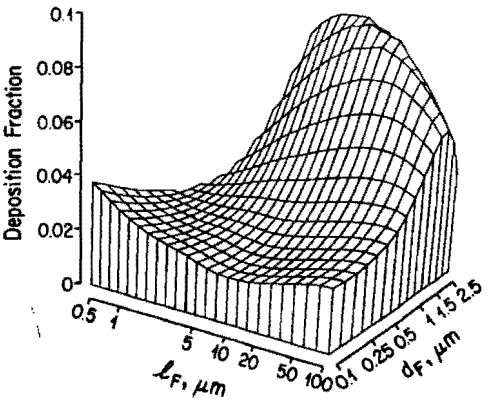

Fig. 7. Pulmonary deposition via trachea at a lung volume of 10.78 cm^3, a tidal volume of 1.68 cm^3, a breathing frequency of 98 cycles min^{-1} and $\rho = 3.37\ g\,cm^{-3}$.

Pulmonary deposition when the interceptional deposition is included is shown in Fig. 7. Despite the higher filtration effect of the tracheobronchial region for long fibers, deposition of these fibers in the pulmonary region may still take place. The filtration effect of the tracheobronchial region causes an overall decrease in deposition in the pulmonary region for all fiber sizes. Figure 7 also shows that the deposition fraction for short and thick fibers in the pulmonary region is larger.

Figure 8 shows the results of pulmonary deposition via nose breathing. The deposition

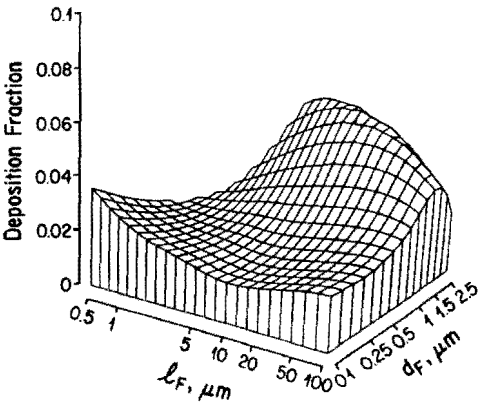

Fig. 8. Pulmonary deposition via nose breathing at a lung volume of 10.78 cm^3, a tidal volume of 1.68 cm^3, a breathing frequency of 98 cycles min^{-1} and $\rho = 3.37\ g\,cm^{-3}$.

pattern with respect to the fiber dimension is similar to Fig. 7 except that the amount is lower due to the additional filtration of the nose.

It should be mentioned that the calculated deposition fraction in the pulmonary region varies strongly with the values of tidal volume and lung volume chosen in the calculation. For the same lung volume, deposition increases with increasing tidal volume; if the tidal volume is kept constant, the deposition fraction will increase with decreasing lung volume.

COMPARISONS WITH EXPERIMENTAL DATA

A considerable amount of experimental deposition data in the rat lung is available for polydisperse fibers. In order to compare the calculated deposition results with these data, we must generalize the model to account for fiber size distributions. Let us consider a polydisperse fiber which has a size distribution function $f(d_f, l_f)$ in diameter and length, the mass fraction of deposition, DE_m, is then determined from the equation

$$DE_m = \frac{\int_0^\infty \int_0^\infty (DE) d_f^2 l_f f(d_f, l_f)\, d(d_f)\, dl_f}{\int_0^\infty \int_0^\infty d_f^2 l_f f(d_f, l_f) d(d_f)\, dl_f}, \tag{28}$$

where DE is the number fraction deposition of a monodisperse fiber of diameter of d_f and l_f. A special case of the polydisperse fiber is when all the fibers have the same aspect ratio. In this case, equation (28) reduces to

$$DE_m = \frac{\int_0^\infty (DE) d_f^3 f(d_f) d(d_f)}{\int_0^\infty d_f^3 f(d_f)\, d(d_f)}. \tag{29}$$

Assuming a lognormal distribution of d_f in the form

$$f(d_f) = \frac{1}{\sqrt{2\pi} d_f \ln \sigma_g} \exp\left\{ -\frac{(\ln d_f - \ln \bar{d}_f)^2}{2 \ln^2 \sigma_g} \right\}, \tag{30}$$

where $\bar{d}_f$ is the count median diameter of the fiber and σ_g is the geometric standard deviation, equation (29) can be written as

$$DE_m = \frac{1}{\sqrt{2\pi} \ln \sigma_g} \int_0^\infty DE(e^y) \exp\left\{ -\frac{[y - (\ln \bar{d}_f + 3 \ln^2 \sigma_g)]^2}{2 \ln^2 \sigma_g} \right\} dy, \tag{31}$$

where

$$y = \ln d_f. \tag{32}$$

Equation (31) has been used to calculate total and pulmonary deposition of a polydisperse fiber. Figures 9 and 10 show the results for a tidal volume of 3 cm^3 and a lung volume of 10.78 cm^3 at different values of equivalent mass diameter, $d_{em} = d_f \beta^{1/3}$ ($\rho = 3.37$ g cm^{-3}) and $\sigma_g = 2$ and the comparisons of these results with the data of Morgan *et al.* (1977). In Morgan's experiments, seven different asbestos fibers were used which had a value of $\bar{d}_f$ ranging from 0.19 to 0.46 μm. The geometric standard deviations for these fibers were in the range of 2–2.7 for length and 1.9–3 for diameter. Since the correlation between the fiber length and diameter was not reported we assume a fiber size distribution with constant aspect ratio and calculate deposition using equation (31). It is seen from Figs 9 and 10 that the calculated results agree reasonably with the data, and in this fiber size range, total deposition increases with d_{em} while the pulmonary deposition remains almost constant.

Hammad *et al.* (1982) used glass fibers ($\rho = 2.5$ g cm^{-3}) of a wide size range to study the pulmonary deposition of fibers in rats. The size distribution of their fibers is shown in Fig. 11 and the corresponding pulmonary deposition data measured after five days of exposure are shown in Fig. 12 in which the relative deposition is the deposition fraction at a given fiber

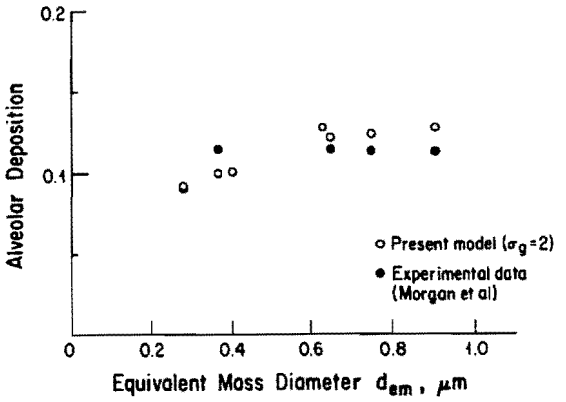

Fig. 9. Comparison of the calculated pulmonary deposition with the experimental data of Morgan *et al.* (1977). The lung volume and the tidal volume in the calculation were, respectively, 10.78 and 3 cm^3.

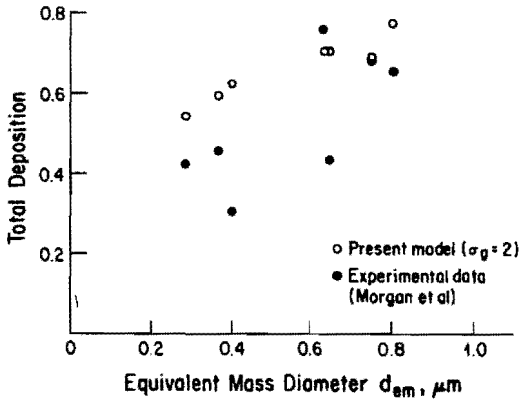

Fig. 10. Comparison of the calculated total deposition with the experimental data of Morgan *et al.* (1977). The lung volume and the tidal volume in the calculation were, respectively, 10.78 and 3 cm^3.

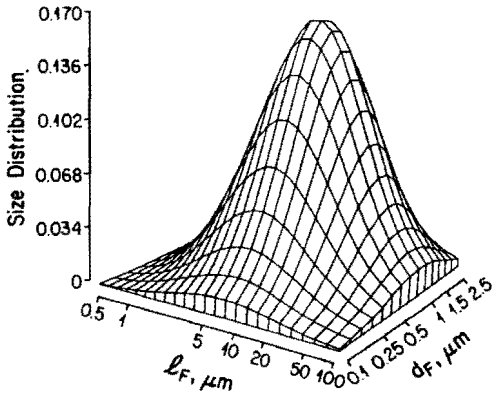

Fig. 11. Bivariate size distribution of glass fibers used in the exposure experiment by Hammad *et al.* (1982).

size vs the maximum deposition fraction. It is seen that deposition occurs at about 0.5 μm fiber diameter and 7 μm fiber length for the size distribution of inhaled fibers studied. The calculated relative deposition is shown in Fig. 13, obtained by multiplying the size distribution shown in Fig. 11 with the deposition efficiency shown in Fig. 8. The calculation was based on a tidal volume of 1.68 cm^3 and a respiratory frequency of 98 cycles min^{-1}.

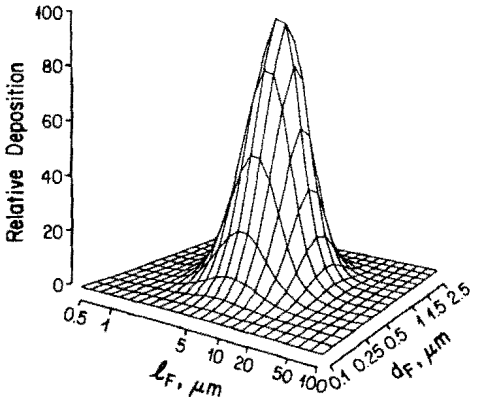

Fig. 12. Bivariate distribution of fiber retention obtained by Hammad *et al.* (1982).

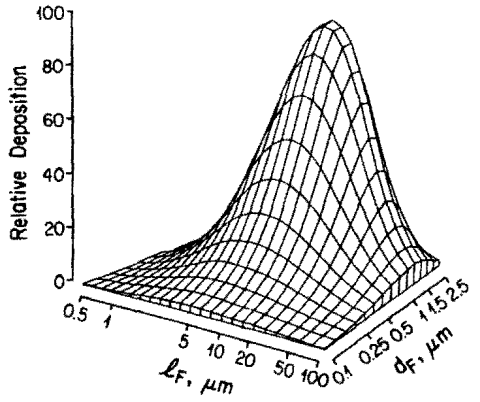

Fig. 13. Bivariate distribution of fiber deposition in the pulmonary region calculated from the present study. The calculation was based upon a lung volume of 10.78 cm^3, a tidal volume of 1.68 cm^3, and a respiratory frequency of 98 cycles min^{-1}.

Figure 13 shows a similar deposition pattern to the data in Fig. 12; the maximum deposition occurs at about 7 μm fiber length but at a slightly larger fiber diameter.

CONCLUSIONS

We have formulated a deposition model for fibers in the rat lung. The calculated results from this model show that deposition pattern depends on both fiber diameter and length. It is also shown that although inhaled fibers are effectively filtered by the nose and the tracheobronchial region due to the mechanisms of interception and impaction, a significant fraction of long fibers can still penetrate into the pulmonary region and deposit.

Acknowledgement—This work was supported by Grant No. HL-38503 from the National Heart, Lung and Blood Institute.

REFERENCES

Allen, M. D. and Raabe, O. G. (1985) *Aerosol Sci. Technol.* **4**, 269–286.
Asgharian, B. and Yu, C. P. (1988a) *J. Aerosol Medicine* **1**, 37–50.
Asgharian, B., Yu, C. P. and Gradon, L. (1988b) *Aerosol Sci. Technol.* **9**, 213–219.
Asgharian, B. and Yu, C. P. (1989) *Aerosol Sci. Technol.* (in press).
Davis, J. M. G., Beckett, S. T., Bolton, R. E., Collings, P. and Middleton, A. D. (1978) *Br. J. Cancer* **37**, 673–688.
Hammad, Y., Diem, J., Craighead, J. and Weill, H. (1982) *Ann. occup. Hyg.* **26**, 179–187.
Morgan, A., Evans, J. C. and Holmes, A. (1977) *Inhaled Particles* IV (Edited by Walton, W. H. and Mcgovern, B.). Pergamon Press, Oxford.

Perterlin, A. (1938) *Z. Phys.* **111**, 232–263.
Pinkerton, K. E., Pratt, C. P., Brody, A. R. and Crapo, J. D. (1984) *Am. J. Pathol.* **117**, 484–498.
Raabe, O. G., Yeh, H. C., George, J. N., Phalen, R. F. and Velasquez, D. J. (1975) *Inhaled Particles* IV (Edited by Walton, W. H. and Mcgovern, B.). Pergamon Press, Oxford.
Schum, M. and Yeh, H. C. (1980) *Bull. math Biol.* **42**, 1–15.
Wagner, J. C., Berry, B., Skidmore, J. W. and Timbrell, V. (1974) *Br. J. Cancer* **29**, 252–269.
Weibel, E. R. (1963) *Morphometry of the Human Lung.* Academic Press, New York.
Yeh, H. C. (1980) *Respiratory Tract Deposition Models.* Inhalation Toxicology Research Institute, Lovelace Biomedical and Environmental Research Institute, Albuquerque, New Mexico.
Yu, C. P., Asgharian, B. and Yen, B. M. (1986) *Am. ind. Hyg. Ass. J.* **47**, 72–77.
Yu, C. P. and Diu, C. K. (1983) *J. Aerosol Sci.* **14**, 599–609.